Mangicols: Structures and Biosynthesis of A New Class of Sesterterpene Polyols from a Marine Fungus of the Genus *Fusarium*

Matthew K. Renner, Paul R. Jensen, and William Fenical*

Center for Marine Biotechnology and Biomedicine, Scripps Institution of Oceanography, University of California−San Diego, La Jolla, California 92093-0204

wfenical@ucsd.edu

Received January 20, 2000

A marine fungal isolate, tentatively identified as *Fusarium heterosporum*, has been found to produce a series of structurally novel sesterterpene polyols, the mangicols A−G (**4**−**10**). The structures of the new compounds, including the stereochemistry of mangicol A, were assigned by interpretation of spectral data derived from both natural products and synthetic derivatives. The mangicols, which possess unprecedented spirotricyclic skeletal components, show only weak to modest cytotoxicities toward a variety of cancer cell lines in in vitro testing. Mangicols A and B, however, showed significant antiinflammatory activity in the PMA (phorbol myristate acetate)-induced mouse ear edema model. A biosynthetic pathway for the neomangicol and mangicol carbon skeletons is proposed on the basis of the incorporation of appropriate radiolabeled precursors.

Introduction

Marine microorganisms, including marine fungi, represent an underdeveloped and potentially prolific source of structurally diverse secondary metabolites.[1] In our research program, we have focused considerable attention on marine fungi, which have been shown to produce novel metabolites with antibiotic[2] and antitumor[3] properties.[4] Recently, we reported the isolation of the neomangicols (**1**−**3**),[5] a series of cytotoxic, halogenated sesterterpenoids obtained from a marine *Fusarium* species tentatively identified a *Fusarium heterosporum* (*F. heterosporum*, Chart 1). The neomangicols are a new class of sesterterpenoids with unprecedented carbon skeletons. From the same organism, we have now isolated a new family of sesterterpenes possessing a related but equally intriguing carbon skeleton. These new compounds, named mangicols A−G (**4**−**10**),[6] which possess novel spirotricyclic structure components, constitute a new class within the C_{25} terpenoids (Chart 1). Like the neomangicols, several mangicols display cytotoxicity against human tumor cell lines. Mangicols A and B (**4, 5**) showed significant antiinflammatory activity in the PMA-induced (PMA - phorbol myristate acetate) mouse ear edema assay.

Results and Discussion

Fusarium strain CNC-477 was isolated from a driftwood sample collected from a mangrove habitat at Sweetings Cay, Bahamas, in 1995. The fungal isolate was cultured in a seawater-based medium, and the fungal broth and mycelium were extracted separately. Bioassay-guided fractionation of the mycelium extract led to the isolation of the neomangicols (**1**−**3**), the structures of which were reported earlier. These fractions also yielded a second family of closely related compounds, mangicols A−G (**4**−**10**), which were subsequently purified by C-18 flash chromatography, Sephadex LH-20 chromatography, silica flash chromatography, and reversed-phase C-18 HPLC. We report here the complete details of the isolation and structure determination of these new compounds.

The HRFABMS (high-resolution fast atom bombardment mass spectral) data derived for mangicol A (**4**) indicated this molecule possessed the molecular formula $C_{25}H_{42}O_5$. The ^{1}H NMR spectrum of **4** in acetone-d_6 (Table 1) showed one olefinic proton, ten protons between δ 3.3 and 4.4, five methyl groups, and sixteen highly coupled protons between δ 1.2 and 2.4, features consistent with a polycyclic terpenoid structure similar to that of neomangicol A (**1**). The ^{1}H NMR spectrum of **4** in methanol-d_4 showed five protons between δ 3.3 and 3.9 indicative of multiple hydroxyl functionalities. These findings were consistent with the strong hydroxyl absorption observed in the IR spectrum.

The ^{13}C NMR spectrum of **4** (Table 2) showed two olefinic carbons, five oxygenated carbons, and eighteen

(1) (a) Pietra, F. *Nat. Prod. Rep.* **1997**, *14*, 453. (b) Fenical, W. *Chem. Rev.* **1993**, *93*, 1883. (c) Davidson, B. S. *Curr. Opin. Biotechnol.* **1995**, *6*, 284. (d) Liberra, K.; Lindequist, U. *Pharmazie* **1995**, *50*, 583.

(2) (a) Poch, G. K.; Gloer, J. B. *J. Nat. Prod.* **1991**, *54*, 213. (b) Abrell, L. M.; Borgeson, B.; Crews P. *Tetrahedron Lett.* **1996**, *37*, 8983. (c) Xu, X. M.; Deguzman, F. S.; Gloer, J. B.; Shearer, C. A. *J. Org. Chem.* **1992**, *57*, 6700. (d) Poch, G. K.; Gloer, J. B. *J. Nat. Prod.* **1991**, *54*, 213.

(3) (a) Takahashi, C.; Takai, Y.; Kimura, Y.; Numata, A.; Shigematsu, N.; Tanaka, H. *Phytochemistry* **1995**, *38*, 155. (b) Numata, A.; Takahashi, C.; Ito, Y.; Minoura, K.; Yamada, T.; Matsuda, C.; Nomoto, K. *J. Chem. Soc., Perkin Trans 1.* **1996**, *3*, 239. (c) Takahashi, C.; Numata, A.; Matsumura, E.; Minoura, K. Eto, H.; Shingu, T.; Ito, T.; Hasegawa, T. *J. Antibiot.* **1994**, *47*, 1242. (d) Shigemori, H.; Wakuri, S.; Yazawa, K.; Nakamura, T. *Tetrahedron* **1991**, *47*, 8529. (e) Takahashi, C.; Numata, A.; Yamada, T.; Minoura, K.; Enomoto, S.; Konishi, K.; Nakai, M.; Matsuda, C.; Nomoto, K. *Tetrahedron Lett.* **1996**, *37*, 655.

(4) Biabani, M. A. F.; Laatsch, H. *J. Prakt. Chem. (Weinheim, Ger.)* **1998**, *340*, 589.

(5) Renner, M. K.; Jensen, P. R.; Fenical, W. *J. Org. Chem.* **1999**, *63*, 8346.

(6) The name mangicol is derived from the term "mangicolous," which is used to describe microorganisms that grow in mangrove environments. The neomangicols were so named because the mangicol carbon skeleton appears to be a biosynthetic precursor for that of the neomangicols.

10.1021/jo000081h CCC: $19.00
Published on Web 07/13/2000

Chart 1

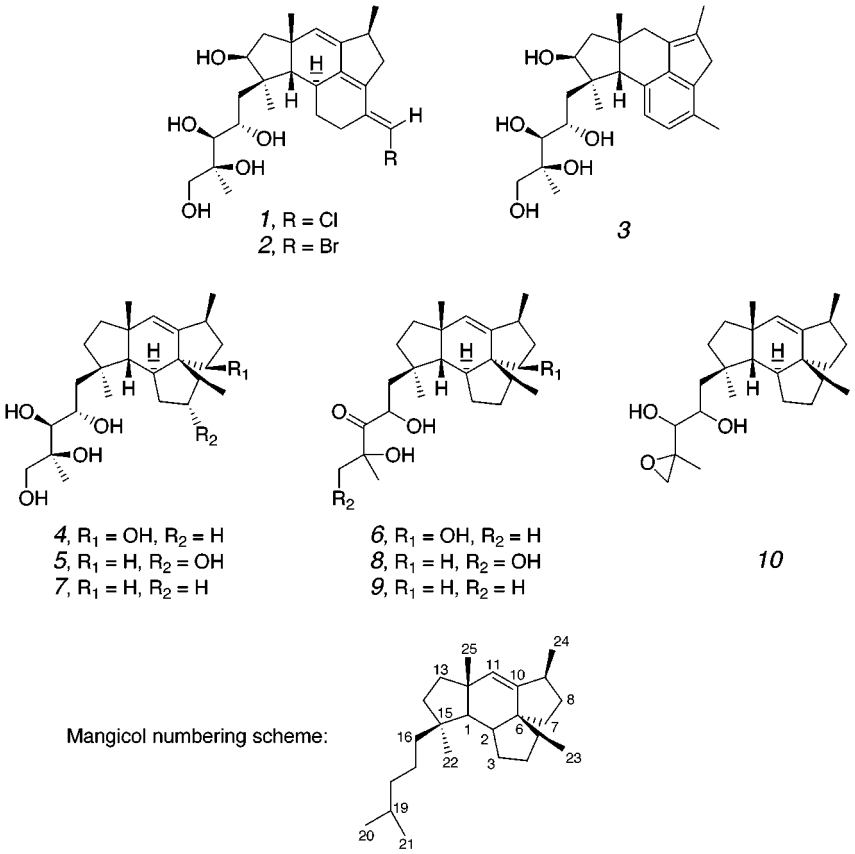

additional carbon signals between δ 19.5 and 59.8. The DEPT (distortionless enhancement by polarization transfer) spectrum indicated five CH_3, seven CH_2, eight CH, and five quaternary carbons. The lack of carbonyl resonances, the presence of only one double bond, and considering the unsaturation equivalent in the molecular formula indicated that mangicol A possessed four rings.

Four substructures of mangicol A (Figure 1) were assigned on the basis of 2D homo- and heteronuclear NMR correlation experiments (Table 3). The considerable structural analogy of **4** to neomangicol A (**1**) aided significantly in the structure assignment for this molecule. Substructure A, for example, was nearly identical to that of **1** except for the lack of a hydroxyl at C-14. Substructure B was assigned on the basis of COSY (correlation spectroscopy) correlations between H-7 and H-8a/H-8b, between H-8b and H-9, and between H-9 and Me-24. The only COSY correlations observed for substructure C were between H-5 and Me-23. The remaining assignments for substructure C were based on HMBC (heteronumclear multiple bond correlation spectroscopy) correlations between the Me-23 protons and carbons C-4, C-5, and C-6. This left only one methylene unaccounted for, and since COSY couplings from these protons were obscured by overlapping proton resonances, this methylene could only be assigned as the isolated fragment, substructure D.

Connection of the mangicol A structure fragments was accomplished primarily by analysis of observed HMBC NMR correlations. Substructures A and B were linked by correlations from H-9 to both C-10 and C-11, from Me-24 to C-10, and from H-11 to C-9. This connection was also indicated by the allylic coupling observed between H-9 and H-11 in the COSY spectrum. Connection of substructures A−C through the quaternary carbon C-6 was established on the basis of numerous HMBC correlations to C-6. The C-6/C-7 connection, for example, was required by HMBC correlations observed from H-7, H-8a, and OH-7 to C-6. Similarly, the C-6/C-10 connection was assigned on the basis of an HMBC correlation from H-11 to C-6, and the C-2/C-6 connection was established on the basis of the HMBC correlation from H-1 to C-6. Finally, the remaining methylene, substructure D, was integrated into the structure on the basis of HMBC correlations from H-3a to C-1, C-4, and C-5, from H-1 to C-3, and from H-4a to C-3. Linking these substructures completed the planar structure assignment for mangicol A.

The relative configurations of the stereocenters of the tetracyclic ring system in mangicol A were assigned on the basis of correlations observed in the NOESY (nuclear Overhauser enhancement spectroscopy) NMR spectrum as well as through interpretation of NMR coupling constant data. Some key NOESY correlations are illustrated in Figure 2.[7] The C-1/C-12 ring junction was assigned as cis on the basis of a strong NOESY correlation observed between H-1 and Me-25. NOESY correlations between H-1 and H-16a established that H-1, C-16, and Me-25 were all spatially oriented on the top face of the molecule. Conversely, strong NOESY correlations between H-2 and Me-22 indicated that Me-22 and H-2 were located on the bottom face. Thus, the relative

(7) The Chem3d structure shown in this figure is the low-energy conformer identified by a Monte Carlo conformation search performed in Macromodel 6.0 using the MM2 force field. This conformer was found 13 times (out of 500 structures processed), and the next lowest-energy conformer was 5.4 kJ/mol higher in energy.

Table 1. ^{1}H NMR Data for the Mangicols A−G (4−10) in Acetone-d_6

no.	mangicol A (4)	mangicol B (5)	mangicol C (6)	mangicol D (7)	mangicol E (8)	mangicol F (9)	mangicol G (10)
1	1.36 (d, 7.2)	1.33 (d, 8.8)	1.37 (d, 7.2)	1.44 (m)	1.48 (m)	1.47 (m)	1.43 (m)
2	1.91 (ddd, 3,7.2,7.2)	1.82 (m)	1.90 (ddd, 2.4,7.2, 7.2)	1.70 (ddd, 2.4,7.2, 9.2)	1.70 (ddd, 1.8,6.6,9)	1.70 (ddd, 2.6,7.6, 9.,5)	1.70 (ddd, 2.4,7.2,9)
3a	2.07 (m)	1.94 (ddd, 1.8,6.5, 12.3)	2.06 (m)	1.87 (m)	1.88 (dddd, 7.2,9,9, 12.6)	1.87 (dddd, 7.2,8.6, 8.6,12.6)	1.88 (dddd, 7.2,9,9, 12.6)
3b	1.44 (m)	1.86 (m)	1.38 (m)	1.59 (m)	1.56 (dddd, 2.4, 3.6, 7.2, 12.6)	1.54 (m)	1.56 (dddd, 2.4, 4.2, 7.8, 12.6)
4a	1.98 (dddd, 4.2, 8.4, 12, 12)	3.95 (dddd, 5.6, 5.6, 7.0, 8.7)	1.98 (m)	1.99 (dddd, 4.2, 8.4, 8.4, 12.6)	1.99 (dddd, 4.2, 8.4, 8.4, 12.6)	1.99 (dddd, 4.2, 8.4, 8.4, 12.6)	1.99 (dddd, 4.2, 8.4, 8.4, 12.6)
4b	1.36 (m)	3.63 (OH, d, 5)	1.36 (m)	1.43 (m)	1.44 (m)	1.45 (m)	1.43 (m)
5	2.37 (m)	1.61 (m)	2.36 (m)	1.79 (m)	1.79 (m)	1.79 (dq, 2.3, 7.5)	1.80 (m)
7a	3.69 (ddd, 6, 6, 12)	2.06 (m)	3.69 (ddd, 6, 6, 10.8)	1.74 (m)	1.74 (m)	1.74 (m)	1.74 (m)
7b	3.80 (OH, d, 5.4)	1.31 (ddd, 6.2, 11.3, 13)	3.84 (OH, d, 4.8)	1.23 (m)	1.23 (m)	1.23 (m)	1.23 (m)
8a	1.94 (m)	1.81 (m)	1.94 (m)	1.83 (m)	1.84 (m)	1.84 (m)	1.84 (m)
8b	1.20 (m)	1.18 (dddd, 5.9, 10, 12.7, 12.7)	1.20 (ddd, 11.4, 12, 12)	1.19 (m)	1.21 (m)	1.22 (m)	1.21 (m)
9	2.39 (m)	2.49 (m)	2.39 (m)	2.51 (m)	2.49 (m)	2.51 (m)	2.50 (m)
11	5.49 (d, 1.2)	5.46 (d, 1.8)	5.49 (d, 1.4)	5.45 (d, 1.2)	5.45 (d, 1.6)	5.44 (d, 1.6)	5.45 (d, 1.8)
13a	1.54 (ddd, 6.6, 12.6, 12.6)	1.51 (ddd, 6.7, 12.4, 12.4)	1.55 (ddd, 6.6, 12, 12)	1.51 (ddd, 6, 12, 12.6)	1.52 (m)	1.51 (m)	1.51 (ddd, 6, 12, 12.6)
13b	1.44 (m)	1.40 (m)	1.46 (m)	1.39 (m)	1.43 (m)	1.42 (m)	1.41 (m)
14a	1.77 (ddd, 6.6, 12, 12)	1.79 (ddd, 5.7, 12, 12.9)	1.94 (m)	1.84 (m)	2.05 (m)	2.01 (m)	1.80 (m)
14b	1.44 (m)	1.41 (m)	1.46 (m)	1.39 (m)	1.43 (m)	1.43 (m)	1.41 (m)
16a	2.03 (d, 14)	2.07 (m)	2.10 (dd, 2.1, 14.4)	2.09 (d, 14.4)	2.16 (dd, 1.4, 14.1)	2.11 (d, 14)	1.85 (dd, 1.5, 14.4)
16b	1.59 (dd, 8.4, 13.8)	1.60 (dd, 8.4, 14.2)	1.46 (m)	1.60 (dd, 8.4, 14.4)	1.46 (m)	1.49 (m)	1.66 (dd, 9, 14.4)
17a	3.90 (ddd, 4.2, 9, 9)	3.90 (ddd, 4.2, 7.8, 8.5)	4.80 (ddd, 1.8, 7.2, 9)	3.90 (ddd, 3.6, 7.8, 8.4)	4.81 (ddd, 1.6, 7.4, 8.8)	4.88 (ddd, 1.5, 7.5, 9)	3.81 (m)
17b	4.31 (OH, d, 3.6)	4.35 (OH, d, 4.1)	3.78 (OH, d, 7.2)	4.37 (OH, s)	3.77 (OH, d, 7.8)	3.81 (OH, d, 7.5)	3.16 (OH, d, 6.6)
18a	3.33 (dd, 5.4, 8.4)	3.33 (dd, 5.8, 8.8)		3.33 (dd, 6, 9)			3.23 (dd, 3, 6)
18b	4.05 (OH, d, 6)	4.11 (OH, d, 5.8)		4.14 (OH, d, 5.4)			3.78 (OH, d, 3)
19	4.39 (OH, s)	4.41 (OH, s)	4.52 (OH, s)	4.46 (OH, s)	4.52 (OH, s)	4.63 (OH, s)	
20a	3.60 (dd, 6, 10.8)	3.60 (dd, 6.5, 10.8)	3.78 (m)	3.60 (d, 10.2)	3.78 (dd, 6.4, 10.8)	1.38 (s)	2.73 (d, 4.8)
20b	3.45 (dd, 4.2, 10.8)	3.44 (dd, 5.1, 10.8)	3.46 (dd, 3.3, 10.8)	3.44 (d, 10.2)	3.46 (dd, 4.8, 10.8)		2.51 (d, 5.4)
20c	3.78 (OH, t, 5.4)	3.79 (OH, dd, 5.3, 6.2)	4.09 (OH, m)	3.86 (OH, br s)	4.09 (OH, dd, 4.8, 6.4)		
21	1.22 (s)	1.22 (s)	1.29 (s)	1.21 (s)	1.30 (s)	1.34 (s)	1.37 (s)
22	0.96 (s)	0.98 (s)	0.99 (s)	1.00 (s)	1.04 (s)	1.04 (s)	1.00 (s)
23	0.87 (d, 7.2)	0.92 (d, 7.5)	0.86 (d, 7.2)	0.86 (d, 7.2)	0.86 (d, 7.2)	0.85 (d, 7.4)	0.86 (d, 7.2)
24	1.09 (d, 6.6)	1.09 (d, 7.0)	1.09 (d, 6.6)	1.09 (d, 7.2)	1.09 (d, 7.2)	1.09 (d, 7.2)	1.09 (d, 6.6)
25	1.13 (s)	1.10 (s)	1.14 (s)	1.12 (s)	1.14 (s)	1.13 (s)	1.12 (s)

Table 2. ^{13}C NMR Data for Mangicols A−G (4−10) in Acetone-d_6

	A (**4**)	B (**5**)	C (**6**)	D (**7**)	E (**8**)	F (**9**)	G (**10**)
1	59.8	58.8	61.0	58.0	58.1	58.0	58.2
2	46.8	46.1	47.0	47.8	47.8	47.8	47.8
3	34.2	43.0	34.8	33.0	33.0	33.0	33.2
4	35.1	81.5	35.4	33.6	33.5	33.5	33.6
5	34.8	52.7	35.7	42.6	42.5	42.5	42.7
6	59.1	56.2	59.5	57.4	57.4	57.5	57.3
7	82.8	46.0	83.9	45.0	45.0	45.0	45.0
8	40.4	31.9	40.1	31.9	31.9	31.9	31.9
9	34.0	38.4	34.6	38.4	38.4	38.4	38.4
10	143.2	145.7	143.3	145.3	145.2	145.2	145.3
11	133.6	131.6	134.4	131.4	131.3	131.3	131.4
12	44.2	44.8	44.8	45.3	45.6	45.6	45.3
13	40.8	40.5	41.2	40.3	40.3	40.3	40.4
14	38.7	39.0	38.7	39.1	38.9	38.8	39.3
15	46.9	46.7	47.8	46.5	46.9	46.9	46.4
16	50.2	50.6	48.4	51.0	49.3	49.6	49.2
17	72.4	72.3	74.4	72.3	74.2	73.1	71.9
18	75.8	75.8	218.1	75.7	217.7	217.7	77.9
19	76.2	76.2	81.4	76.2	81.1	77.6	58.3
20	69.7	69.7	70.3	69.7	70.0	28.2	51.4
21	19.5	19.5	23.2	19.5	23.3	28.6	18.6
22	24.3	24.6	24.8	24.9	24.8	24.8	24.8
23	21.8	20.1	21.9	22.4	22.5	22.5	22.4
24	21.4	21.2	21.5	22.0	22.0	22.0	22.0
25	31.2	30.9	31.4	30.8	30.7	30.6	30.8

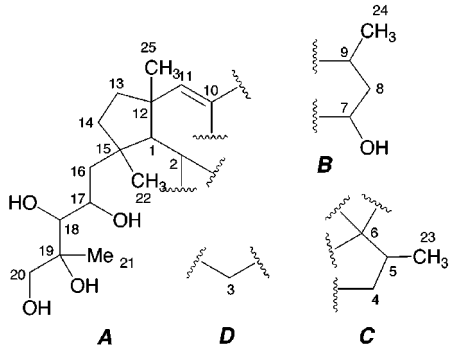

Figure 1. Substructures of mangicol A (**4**).

configurations at C-1, C-2, C-12, and C-15 were shown to be analogous to those in neomangicol A (**1**).

The relative configurations at C-5, C-6, and C-7 could also be assigned on the basis of NOESY correlations involving H-7 and Me-22. NOESY correlations between H-7 and H-2, and between H-7 and Me-22, established that H-7 (and thus C-7) must be on the bottom face of the molecule. A complementary NOESY correlation between Me-23 and Me-25 indicated that C-5 must be on the top face of the mangicol A framework. An additional NOESY correlation between H-5 and OH-7 provided confirming evidence for the assignments of C-5 and C-7. Also, the spatial proximity of H-5 and OH-7, which deshields H-5, provided ample justification for the unusual chemical shift of H-5 at δ 2.37. Finally, a NOESY correlation between Me-23 and Me-24 required that Me-24 be positioned upward on the top face of the molecule.

In the structure elucidation of the previously reported neomangicols, it was possible to assign the absolute configuration at C-14 using the refined Mosher's method.[5,8] To achieve this, the side-chain hydroxyl groups were first selectively protected as bis-acetone ketals; then MTPA esters were prepared at the underivatized C-14 hydroxyl. A similar strategy involving the hydroxyl at C-7 was employed for mangicol A. Treatment of mangicol A (**4**) with 2,2-dimethoxypropane and catalytic camphorsulfonic acid in acetone provided the bis-acetone ketal derivative **11** (Scheme 1). The bis-acetone ketal **11** was then treated, in separate experiments, with (*R*)- and (*S*)-MTPA-Cl to prepare the corresponding diastereomeric Mosher's esters. The *S* ester, **12**, was prepared smoothly under standard conditions, but formation of the *R*-MTPA ester, **13**, was extremely sluggish, requiring higher temperatures and longer duration reaction times to achieve complete conversion.

The difficulty encountered in the preparation of the *R* ester, and the overall hindered environment in proximity of the hydroxyl group, suggested great caution in the interpretation of the results. There was concern that steric hindrance might prevent the MTPA (methoxy-(trifluoromethyl)phenyl acetic acid) ester from adopting the conformation required for successful application of the method. Models of the MTPA esters revealed no destabilizing interactions, however, and the pattern of differential shielding (Figure 3) was consistent with the predicted model for the modified Mosher's method (i.e., all NMR $\Delta\delta$ values negative on one side of the MTPA plane and positive on the other side). More significant, perhaps, is that the absolute configurations predicted by this experiment are identical with the absolute configurations determined for the related neomangicol sesterterpenoids. The predicted absolute configuration, *R*, at C-7 of mangicol A, requires that the configurations of the other stereocenters in the cyclic portion of the molecule be 1*R*, 2*S*, 5*S*, 6*R*, 9*S*, 12*R*, and 15*R*. Where comparable, these are the same configurations observed for neomangicol A.[5,9] It is well-known that the complex cyclic structures characteristic of terpenoid natural products are created by terpene cyclases, single enzymes responsible for converting a linear terpenoid precursor into polycyclic ring systems.[10] It seems likely, given that both are produced by the same fungal strain, that the carbon skeletons of the mangicols and the neomangicols are produced by the same cyclase. Given the complexity observed in the active sites of the other terpene cyclases,[11] it only stands to reason that the absolute configurations of the carbocyclic stereocenters (i.e., C-1, C-2, C-9, C-12, and C-15) would be the same for both the mangicols and the neogmangicols.

The three remaining unassigned stereocenters in mangicol A were present in the side chain. In the structure elucidation of the neomangicols, three different bis-acetone ketal derivatives were prepared. Two of these derivatives involved cyclization of the C-14 hydroxyl. Analysis of those ketal derivatives using NMR and molecular modeling techniques allowed us to assign the configuration of the three side-chain alcohol-bearing stereocenters.[5] Although the four hydroxyls in the side chain of mangicol A are analogous to those in neoman-

(8) (a) Dale, J. A.; Dull, D. L.; Mosher, H. S. *J. Org. Chem.* **1969**, *34*, 2543. (b) Dale, J. A.; Mosher, H. S. *J. Am. Chem. Soc.* **1973**, *95*, 512. (c) Sullivan, G. R.; Dale, J. A.; Mosher, H. S. *J. Org. Chem.* **1973**, *38*, 2143. (d) Ohtani, I.; Kusumi, T.; Kashman, Y.; Kakisawa, H. *J. Am. Chem. Soc.* **1991**, *113*, 4092.

(9) Note that the stereochemical descriptor for C-1 of neomangicol A is *S*. This reflects a different assignment of Cahn−Ingold−Prelog priorities due to the hydroxyl at C-14. The actual orientation of the stereocenter is the same.

(10) Cane, D. E. *Chem. Rev.* **1990**, *90*, 1089.

(11) (a) Wendt, K. U.; Poralla, K.; Schulz, G. E. *Science* **1997**, *277*, 1811. (b) Starks, C. M.; Back, K.; Chappell, J.; Noel, J. P. *Science* **1997**, *277*, 1815. (c) Lesburg, C. A.; Zhai, G.; Cane, D. E.; Christianson, D. W. *Science* **1997**, *277*, 1820.

Table 3. HMBC Data for Mangicols A−G (4−10) in Acetone-d_6

^{1}H	A (**4**)	B (**5**)	C (**6**)	D (**7**)	E (**8**)	F (**9**)	G (**10**)
1	2, 3, 6, 11, 12, 13, 15, 16, 22, 25	3, 11, 12, 13, 15, 16, 22, 25	2, 3, 11, 12, 13, 14, 16, 22, 25		2, 3, 12, 13, 16, 22, 25	3, 11, 12, 13, 16	
2	1, 4, 5, 7, 15		1, 3, 4, 7, 15	1, 3, 4, 5, 7, 15, 16	1, 4, 5, 7, 15	1, 4, 5, 7, 12, 15	1, 4, 5, 6, 7, 15
3a	1, 4, 5	1, 2, 4, 5, 6	1, 4		1, 2, 4, 5	1, 2, 4, 5	1, 2, 4, 5
3b		1, 2, 4, 5	1, 2, 4, 6	3, 4	2, 5		1, 2, 4, 5, 6
4a	2, 3, 6, 23	6, 23	2, 3, 6, 23	2, 3, 5, 6, 23	2, 3, 5, 6, 23	2, 3, 5, 6, 23	2, 3, 5, 6, 23
4b	5, 23	3, 5	3, 5, 6, 23			5, 23	
5	2, 4, 6, 7, 23	2, 4, 6, 7, 23	2, 3, 4, 6, 7, 23	2, 3, 6, 7, 23	2, 6, 7, 23	2, 6, 7, 23	
7a	2, 5, 6, 8, 9	5, 6, 9, 10	2, 5, 6, 8	5, 6, 8, 9, 10	5, 6, 8, 9, 10	5, 6, 8, 9, 10	5, 6, 8, 9, 10
7b	6, 7, 8	2, 5, 6, 8	6, 7, 8	2, 5, 6, 8	2, 5, 6, 8	2, 5, 6, 8	2, 5, 6, 8
8a	6, 7, 9.10				6, 7, 9, 10	6, 7, 9, 10	
8b	7, 9, 24	7, 9, 24	6, 7, 9, 24	7, 9	5, 7, 9, 24	7, 9, 24	7, 9
9	8, 10, 11, 24	8, 10, 11, 24	8, 10, 11, 24	6, 8, 10, 11, 24	6, 8, 10, 11, 24	6, 8, 10, 11, 24	8, 10, 11, 24
11	1, 6, 9, 12, 13, 24, 25	1, 6, 9, 12, 13, 24, 25	1, 6, 9, 12, 13, 24, 25	1, 6, 9, 12, 13, 24, 25	1, 6, 9, 12, 13, 24, 25	1, 5, 6, 9, 12, 13, 24, 25	1, 6, 9, 12, 13, 24, 25
13a	11, 12, 14, 25	11, 12, 14, 25	11, 12, 14, 15, 25	11, 12, 14, 25	11, 12, 14, 25	12, 14, 25	11, 12, 14, 25
13b							
14a	13, 15, 16, 22	13, 15, 16, 22			13, 15, 16, 22	13, 15, 16, 22	
14b							
16a	1, 14, 15, 17, 18, 22	1, 14, 15, 17, 18, 22	1, 14, 15, 17, 18, 22	1, 14, 15, 17, 18, 22	1, 14, 15, 17, 18, 22	1, 14, 15, 18, 22	14, 15, 17, 18, 22
16b	1, 14, 15, 17, 18, 22	1, 14, 15, 17, 18, 22		1, 14, 15, 17, 18, 22		1, 14, 18, 22	1, 14, 15, 17, 18, 22
17a	15, 16, 18	15, 16, 18	15, 16, 18	15, 16, 18	15, 16, 18	15, 16, 18	15, 16, 18, 19
17b	16, 17, 18	16, 17, 18	16, 17, 18	16, 17, 18	16, 17, 18	16, 17, 18	16, 17, 18
18a	16, 17, 19, 20, 21	16, 17, 19, 20, 21		16, 17, 19, 20, 21			16, 18, 19, 20, 21
18b	17, 18, 19	17, 18, 19		17, 18, 19			17, 18
19	18, 19, 20	18, 19, 20, 21	18, 19, 20, 21	18, 19, 20, 21	18, 19, 20, 21	18, 19, 20, 21	
20a	18, 19, 21	18, 20, 21	21	18, 19, 21	18, 19, 21	18, 19, 21	18, 19, 21
20b	18, 19, 21	18, 19, 21	18, 19, 21	18, 19, 21	18, 19, 21		18, 19, 21
20c	19, 20	19, 20	19, 20		19, 20		18, 19, 20
21	18, 19, 20	18, 19, 20	18, 19, 20	18, 19, 20	18, 19, 20	18, 19, 20	18, 19, 20
22	1, 14, 15, 16	1, 14, 15, 16	1, 14, 15, 16	1, 14, 15, 16	1, 14, 15, 16	1, 14, 15, 16	1, 14, 15, 16
23	4, 5, 6	4, 5, 6	4, 5, 6	4, 5, 6	4, 5, 6	4, 5, 6	4, 5, 6
24	8, 9, 10	8, 9, 10	8, 9, 10	8, 9, 10	8, 9, 10	8, 9, 10	8, 9, 10
25	1, 11, 12, 13	1, 11, 12, 13	1, 11, 12, 13	1, 11, 12, 13	1, 11, 12, 13	1, 11, 12, 13	1, 11, 12, 13

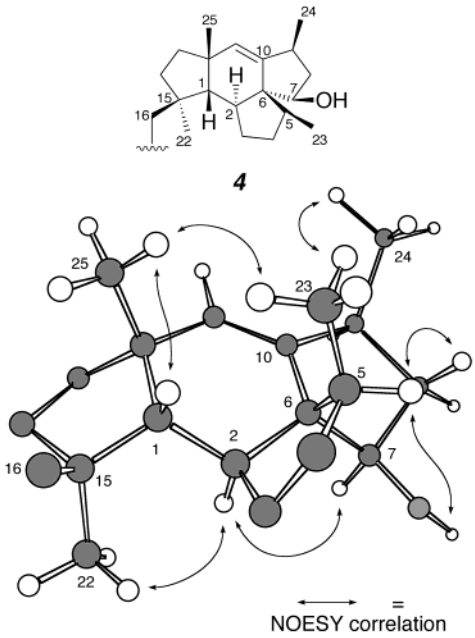

Figure 2. Chem3D representation of the global minimum conformation (Macromodel, MM2 force field, Monte Carlo conformation search) of mangicol A (**4**).

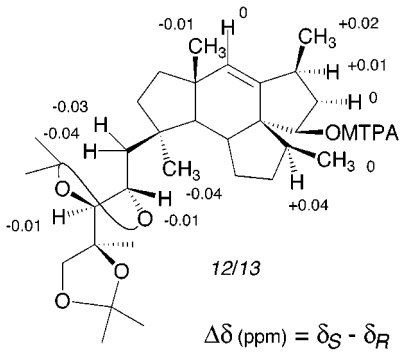

Figure 3. Mosher ester analysis of bis-acetone ketal **11**.

Scheme 1

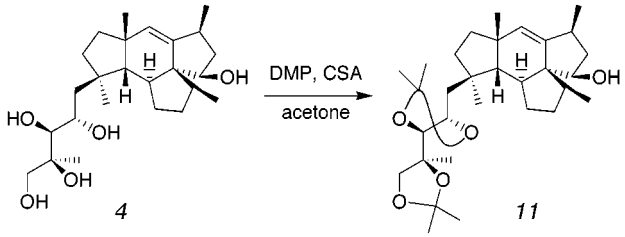

gicol A, the fifth hydroxyl is located at C-7, not C-14, a location too distant to form an acetone-ketal derivative with a side-chain hydroxyl group. On its own, the NMR data obtained for bis-acetone ketal **11** were insufficient to assign the side-chain stereochemistry. Comparison of these data to that observed for the analogous bis-acetone ketal derivative of neomangicol C (**14**) (Table 4), however, led to the conclusion that the relative stereochemistry is the same for the three chiral centers on both side chains. Comparison of the ^{13}C NMR shifts of neomangicol A (**1**) and mangicol A (**4**) supported this conclusion.

Mangicol B (**5**) also analyzed for $C_{25}H_{42}O_5$ by HR-FABMS and combined spectral methods. While the ^1H and ^{13}C NMR spectra for mangicols A and B appeared

Table 4. ^{13}C NMR Data for Mangicol A (4), Neomangicol A (1), and Diacetonide Derivatives (11, 14)

carbon	**4**, acetone-d_6	**1**, methanol-d_4	**11**, $CDCl_3$	**14**, $CDCl_3$
16	50.2	43.0	42.7	42.1
17	72.4	71.0	75.5	75.4
18	75.8	75.9	81.0	81.0
19	76.2	76.8	81.7	81.6
20	69.7	69.3	74.7	74.6
21	19.5	19.5	21.4	21.0
26			109.8	110.2
29			107.1	107.8

very similar, the difference between the two compounds became obvious by interpretation of 2D NMR data. The western half of mangicol B (including the side chain) was found to be identical to that of mangicol A. As in mangicol A, four hydroxyl groups were assigned on the side chain. It was apparent that the fifth hydroxyl was not located at C-7 because its methine proton (geminal to the hydroxyl) appeared as a sixteen line multiplet at δ 3.95 (instead of an eight line multiplet, as in **4**). To achieve this additional coupling, the hydroxyl must be located at C-3, C-4, or C-8. HMBC correlations from the hydroxyl methine proton to C-6 and C-23, and from the hydroxyl proton to C-3, C-4, and C-5, allowed assignment of the hydroxyl group at C-4. This assignment was confirmed by HMBC correlations to the C-4 hydroxyl carbon from its neighboring protons at H-3a, H-3b, H-5, and Me-23.

The remaining difference between the ^1H NMR spectra for **4** and **5**, the chemical shift for H-5, was also explained by the location of the hydroxyl group. In **4**, H-5 (δ 2.37) was deshielded due to spatial proximity to the hydroxyl oxygen at C-7. This was not the case in **5**; H-5 was observed at δ 1.61.

The relative configurations of the stereocenters in **5** were assigned on the basis of correlations observed in the NOESY NMR spectrum. In particular, H-4 showed NOESY correlations with H-1, Me-23, and Me-24, consistent with its location on the top face of the molecule. NOESY data showed that the relative configurations of the remaining stereocenters in **5** were the same as that found in mangicol A (**4**).

The molecular formula of mangicol C (**6**) was assigned as $C_{25}H_{40}O_5$ on the basis of HRFABMS and 1D and 2D NMR data. Assignment of the structure for this metabolite was again aided by the considerable structural analogy to mangicol A. NMR data showed that **6** possessed the identical tetracyclic ring system as in **4**. The only significant variations in the ^1H NMR spectra between mangicols A and C were the disappearance of signals for H-18 and OH-18, the downfield shift of H-17 (from δ 3.90 to δ 4.80), and the upfield shift of OH-17 (from δ 4.31 to δ 3.78). The ^{13}C NMR spectrum for **6** showed only four oxygenated carbons (δ 83.1 to δ 69.9), as well as one carbonyl band with a chemical shift appropriate for that of a ketone (δ 218.2). The lack of proton signals assignable at C-18 indicated the location of the ketone at this position in the side chain. The C-18 assignment was confirmed by HMBC correlations from its neighboring protons H-16a, H-17, OH-19, H-20b, and Me-21. Unfortunately, data were not obtained to allow assignment of the configurations of the alcohol-bearing carbons at C-17 and C-19.

Mangicol D (**7**) was analyzed for $C_{25}H_{42}O_4$ by HR-FABMS and combined NMR spectral data. Comparison of 1D and 2D NMR data obtained for **7** with those of **4** and **5** quickly revealed that the side chains for all three

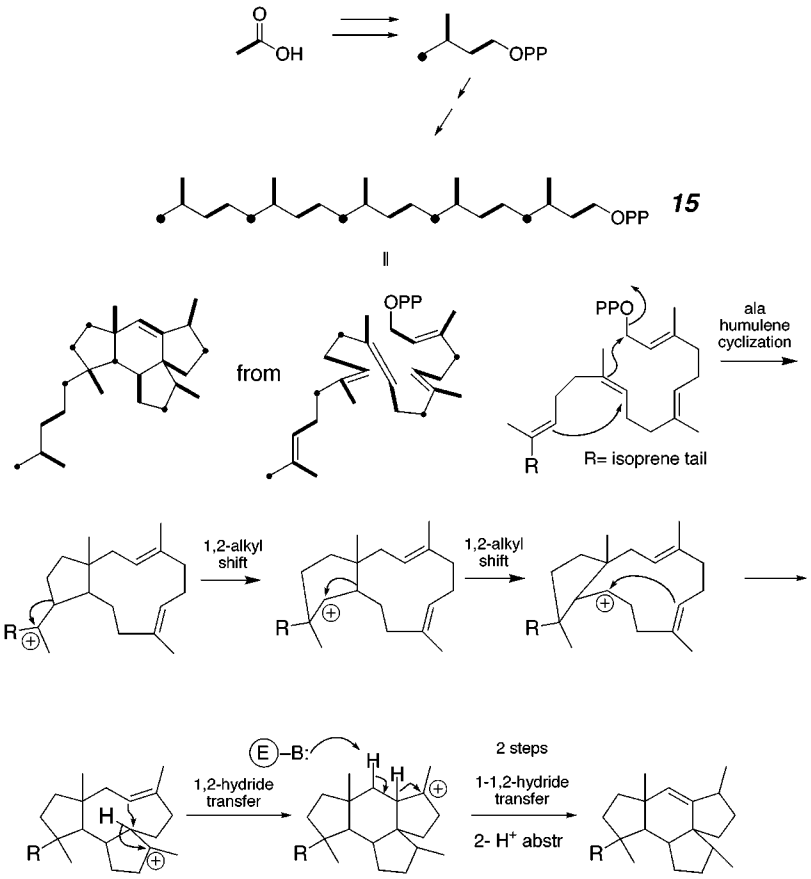

Figure 4. Proposed terpenoid biosynthetic pathway, based upon ^{13}C acetate labeling studies, for the production of the mangicol carbon skeleton.

compounds were identical. The NMR [including HMQC (heteronuclear multiple quantum coherence spectroscopy) and HMBC] data for the cyclic portion of the molecule was consistent with the same carbon skeleton observed for the other mangicols with no hydroxyl groups present. Although data were not obtained to assign the absolute stereochemistry of mangicol D, it seemed reasonable to assume it to be identical to mangicol A (**4**).

The remaining three mangicols were found to differ from mangicol D only in the side chain. NMR comparison clearly showed that the cyclic portions of the molecules were identical. The molecular formula of mangicol E (**8**) was assigned as $C_{25}H_{40}O_4$ on the basis of HRFABMS data. The ^1H, ^{13}C, and HMBC NMR data observed for protons and carbons in the side chain of mangicol E (**8**) were nearly identical to those observed for mangicol C (**6**). Thus, the side chain in mangicol E was assigned with a ketone at C-18 and hydroxyl groups at C-17, C-19, and C-20. As in mangicol C, no data were obtained to suggest the relative nor absolute configurations of the hydroxyl-bearing carbons, C-17 and C-19.

The molecular formula of mangicol F (**9**) was assigned as $C_{25}H_{40}O_3$ on the basis of HRFABMS and combined spectral data. The ^{13}C NMR data indicated that the three oxygen atoms in the molecular formula were present as two hydroxyl groups and one ketone. Unlike the previous mangicols, the presence of six methyl groups in mangicol F, rather than five, suggested that C-20 was not hydroxylated. These suspicions were confirmed through analysis of the 2D NMR data (COSY, HMQC, and HMBC) for **9**, which showed, as in mangicols C (**6**) and E (**8**), that the ketone was positioned at C-18 and hydroxyl groups were located at C-17 and C-19. Like the other ketone derivatives, the stereochemistries at C-17 and C-19 could not be assigned.

Mangicol G (**10**) also analyzed for $C_{25}H_{40}O_3$ on the basis of HRFABMS data. Since no carbonyl or additional olefinic (other than C-10 and C-11) signals were observed in the ^{13}C NMR spectrum of this molecule, the presence of a fifth ring was indicated. The upfield shift observed for the C-20 protons (δ 2.73 and 2.51 verses δ 3.60 and 3.45 for **4**) was suggestive of a terminal epoxide. The ^{13}C NMR shifts for C-19 and C-20 (δ 58.3 and 51.4) and analysis of 2D NMR data (COSY, HMQC, and HMBC) confirmed this assignment. Unfortunately, lack of material precluded our further probing the stereochemistry of the three contiguous chiral centers, C-17 through C-19.

Biosynthesis of the Mangicols and Neomangicols. A simple glance at the mangicol and neomangicol carbon skeletons, especially the spacing of methyl substitution, leads to the reasonable conclusion that they are of terpenoid origin. Ruzicka's biogenetic "Isoprene Rule" postulates that terpenes are compounds formed of linear ("head-to-tail") combinations of isoprene units.[12] Thus, the typical biogenetic precursor for the C_{25} sesterterpenes is geranylfarnesyl diphosphate (**15**, Figure 4).

It is possible to dissect the mangicol and neomangicol carbon skeletons into separate isoprene units, but none of the possible dissections suggests head-to-tail arrangements or even a $C_{10} + C_{15}$ head-to-head arrangement. Thus, it appears that the mangicol carbon skeleton is produced by an unknown skeletal rearrangement during

(12) Ruzicka, L. *Proc. Chem. Soc.* **1959**, 541.

Table 5. Biosynthetic Feeding Experiment Results: ^{13}C NMR Chemical Shifts, Coupling Constants, and Specific Incorporations[14] for Mangicol A and Neomangicol A

	mangicol A (**4**)				neomangicol A (**1**)			
			incorp				incorp	
carbon	δ (ppm)	$J_{C,C}$ (Hz)	feeding 1	feeding 2	δ (ppm)	$J_{C,C}$ (Hz)	feeding 1	feeding 2
1	59.8		0.75	0.31	55.4		0.77	0.42
2	46.8	35	0.96	0.34	32.0	33	0.87	0.37
3	34.2	31	0.83		34.5	33	0.80	
4	35.1		0.72	0.49	28.7		0.82	0.44
5	34.9	37	0.88		138.2	81	0.74	
6	59.1	37	0.97	0.29	133.0	65	0.81	
7	82.8	37	0.76		144.5	65	0.88	0.44
8	40.4		0.82	0.43	39.8		0.75	0.45
9	34.1	34	0.86		36.6	36	0.78	
10	143.2	72	0.84	0.33	146.5	72	0.82	0.32
11	133.6	72	0.64		128.2	72	0.78	
12	44.2	37	0.94		43.9	35	0.70	
13	40.8		0.78	0.46	47.6		0.75	0.49
14	38.7		0.75		80.0		0.76	
15	46.9	38	0.84		52.3	35	0.84	
16	50.2		0.78	0.47	42.9	0	0.77	0.51
17	72.4	42	0.70		71.0	43	0.76	
18	75.9	40	0.77	0.30	75.9	43	0.89	0.42
19	76.2	40	0.99		76.8	40	0.85	
20	69.7		0.75	0.40	69.3		0.80	0.49
21	19.5	40	0.66	0.32	19.5	39	−0.73	0.34
22	24.3	36	0.89	0.30	21.5	35	0.90	0.42
23	21.8	37	0.82	0.52	112.6	81	0.83	0.35
24	21.4	36	0.75	0.44	18.5	36	0.85	0.37
25	31.2	36	0.86	0.30	35.5	35	0.94	0.39

biosynthesis. One of the most precedented terpenoid modifications, a biosynthetic methyl migration, seemed a likely explanation: migration of a methyl group from C-1 to C-12 during cyclization leads to an intermediate which could arise from **15** (i.e., an all head-to-tail arrangement). On the basis of this hypothesis, we set out to investigate the biosynthesis of the mangicols and neomangicols by feeding isotopically labeled precursors. Two feeding studies were performed, the first with sodium [1,2-^{13}C]acetate and the second with sodium [1-^{13}C]acetate. Fungal strain CNC-477 (*Fusarium* cf. *heterosporum*) was grown in 3 L volumes in a seawater-based medium containing yeast extract (15 g), peptone (15 g), glucose (3 g), and the labeled sodium acetate (300 mg for feeding experiment 1, 250 mg for feeding experiment 2). The fermentations were undertaken in a fashion identical to that described for the production of **4**−**10**. Mangicol A and neomangicol A were isolated and purified from the mycelium extract and analyzed using ^{13}C NMR methods. Incorporation of the labeled precursors is summarized in Table 5.

The results of feeding experiment 1 showed that all twenty-five carbons were labeled to approximately the same degree (specific incorporation ~ 0.81%),[13] consistent with the predicted biosynthesis from a C_{25} precursor (geranylfarnesyl diphosphate) (**15**). The incorporation pattern observed clearly precluded the methyl migration originally postulated: all five methyl groups were incorporated intact with their acetate partners. The observed labeling pattern indicated that three of the five isoprene units were incorporated intact (acetate is incorporated into terpenes in a characteristic pattern—see Figure 4). One of these intact isoprene units (C-17 through C-21) comprised the tail of the C_{25} terpene. The second (C-4 through C-7 plus C-23) and third (C-8 through C-11 plus C-24) intact isoprene units appeared to constitute the other end of the C_{25} unit. The remaining two isoprene units were rearranged such that C-1 appeared to have been inserted into an isoprene composed of C-13, C-12, C-25, C-2, and C-3.

A hypothetical biosynthesis accounting for these observations is proposed in Figure 4. The initial cyclization to give an eleven-membered ring is analogous to the biosynthesis of the humulene skeleton and has been observed in another fungal terpenoid.[14] Two Meerwein (1,2-alkyl) shifts are proposed to account for the rearrangement in the carbon skeleton. The remaining steps are simple cation-induced ring closures and 1,2-hydride transfers.

The labeling pattern observed for the neomangicol carbon skeleton is nearly identical to that observed for the mangicols, reinforcing their obvious relationship. The labeling pattern for neomangicol, however, is not contiguous through carbons C-6−C-8 indicative that the neomangicol carbon skeleton is derived from a mangicol skeleton precursor. One feasible explanation would be a 1,2-alkyl shift from a C-7 carbocation in the mangicol skeleton to generate the more stable tertiary carbocation at C-6. This rearrangement, and subsequent modifications, including chlorination and bromination could lead to the production of neomangicols A and B.

The structures of the mangicols represent a unique, new class of sesterterpenoid metabolites. Their relationship to the previously reported neomangicols A and B now appears clearly understood on the basis of the biosynthetic experiments reported here. The mangicols showed only modest cytotoxicities toward cancer cells in in vitro evaluation. Mangicols A−G showed IC50 values (GI50) ranging from 18 to 36 μM in the National Cancer

(13) Specific incorporation = percent enrichments above natural abundance = 1.1% × (combined peak height of enriched satellites minus the combined theoretical peak height for the same satellites resulting from natural abundance coupling)/(peak height of the natural abundance singlet plus the combined theoretical peak height for all satellites resulting from natural abundance coupling).

(14) Dewick, P. M. *Nat. Prod. Rep.* **1997**, *14*, 111.

Institutes 60 cell line panel (mangicol A, 24.5 μM; mangicol B, 20.4 μM; mangicol C, 17 μM; mangicol D, 24.5 μM; mangicol E, 17.8 μM; mangicol F, 36.3 μM; mangicol G, 25.1 μM). The testing results we obtained did not indicate selectivity against selected cancer cell lines nor sufficient potency to be considered of utility in the treatment of cancer. Perhaps more significantly, mangicols A and C showed considerable inhibition of phorbol myristate acetate-induced edema (inflammation) in the mouse ear edema assay (81 and 57% reduction in edema, respectively) at the standard testing dose of 50 μg per ear. These values are consistent with the potencies of existing antiinflammatory agents in this assay (indomethacin shows 71% reduction) and indicate that the mangicols may be of interest in this therapeutic application.

Fungal strain CNC-477 was tentatively identified as *Fusarium heterosporum*, a typical terrestrial *Fusarium* species, on the basis of its characteristic morphological features and upon the shape of its characteristic "banana-shaped" spores. We question this assignment on the basis of our chemical results, since typical *F. heterosporum* has not been observed to produce this class of metabolites. Studies are now in progress to compare the 18S-rRNA sequence from this strain to a larger database derived from other *Fusarium* species. The results of this study promise to provide more definitive information on this issue.

Experimental Section

General Procedures. Proton NMR spectra were recorded at 600 or 300 MHz, while carbon NMR spectra were recorded at 100 or 75 MHz. All spectra were recorded in acetone-d_6, methanol-d_4, or chloroform-d, and chemical shifts were referenced to either the corresponding solvent signal or tetramethylsilane: δ 2.05 ppm/δ 29.9 ppm, δ 3.31 ppm/δ 49.1 ppm, δ 0.0 ppm/δ 77.0 ppm. The numbers of attached protons on carbon atoms were determined through DEPT experiments, and all carbon assignments made were consistent with the DEPT results. 2D HMBC and HMQC experiments were optimized for $^nJ_{CH} = 8.0$ Hz and $^1J_{CH} = 150.0$ Hz, respectively. HPLC separations were accomplished using a Rainin DYNAMAX-60 Å ODS column (250 × 10 mm) at a flow rate of 2.5 mL/min or a Rainin DYNAMAX-60 Å SiO_2 column (250 × 10 mm) at a flow rate of 3.5 mL/min, both with refractive index detection.

Cultivation, Extraction, and Isolation. In a typical experiment, the fungus was cultured for 21 days without shaking in 20 1 L Fernbach flasks using a nutrient medium prepared from sterile seawater, yeast extract (0.5%), peptone (0.5%), glucose (1%), and crab meal (0.2%). The mycelium and broth were separated by filtration, and each was extracted independently. The mangicols were found only in the mycelium extract. In a typical workup, freeze-dried cells from a 20 L cultivation were extracted with CH_2Cl_2:MeOH (1:1), and the organic extract was concentrated to afford 15.6 g of a brown oil. The oil was first fractionated by C-18 reversed-phase flash chromatography, and the portion eluting between 75:25 MeOH:H_2O and 90:10 MeOH:H_2O (1.53 g) was further fractionated by Sephadex LH-20 chromatography (3:1:1 hexane:toluene:methanol, 0.5 mL/min flow rate, 20 mL fractions). Fractions 8−10 (355 mg) were combined and separated by flash chromatography into three fractions. Fraction 1 (166 mg) was purified by reversed phase HPLC (95:5 MeOH:H_2O) to afford mangicol F (**9**, 35 mg, t_R = 19.5 min). Flash fraction 2 (143 mg) was purified by reversed-phase HPLC (95:5 MeOH:H_2O) to afford mangicol G (**10**, 11 mg, t_R = 19 min). LH-20 fractions 11−13 (134 mg) were combined and separated by flash chromatography into two fractions. Fraction 1 (19 mg) was purified by reversed-phase HPLC (95:5 MeOH:H_2O) to afford mangicol E (**8**, 8 mg, t_R = 17 min) and mangicol G (3 mg). Fraction 2 (96 mg) was purified by normal-phase HPLC (40:60 isooctane:ethyl acetate) to afford mangicol D (**7**, 42 mg, t_R = 18 min). LH-20 fractions 21−28 were combined (140 mg) and separated by flash chromatography into two fractions. Fraction 1 (21 mg) was purifed by normal phase HPLC (40:60 isooctane:ethyl acetate) to afford mangicol C (**6**, 10 mg, t_R = 14.5 min). Flash fraction 2 (116 mg) was purified by reversed-phase HPLC (90:10 MeOH:H_2O) to afford mangicol A (**4**, 72 mg, t_R = 10 min) and mangicol B (**5**, 8 mg, t_R = 12 min).

Mangicol A (4). White crystalline solid; mp 86−88 °C; $[\alpha]_D$ = +80° (*c* 0.20, MeOH); UV λ_{max} (MeOH): 203 nm (ϵ 3000); IR (film): 3362 (br), 2937 (s), 2868 (m) cm^{-1}; HRFABMS: $[M+Cs]^+$ *m*/*z* obsd 555.2109, calcd for $C_{25}H_{42}O_5Cs$ 555.2087. For ^{1}H NMR, ^{13}C NMR, HMQC, and HMBC data, see Tables 1−3.

Mangicol B (5). White amorphous solid; $[\alpha]_D$ = +61° (*c* 0.33, MeOH); UV λ_{max} (MeOH): 203 nm (ϵ 2800); IR (film): 3358 (br), 2942 (s), 2865 (w) cm^{-1}; HRFABMS: $[M+Cs]^+$ *m*/*z* obsd 555.2105, calcd for $C_{25}H_{42}O_5Cs$ 555.2087. For ^{1}H NMR, ^{13}C NMR, HMQC, and HMBC data, see Tables 1−3.

Mangicol C (6). White amorphous solid; $[\alpha]_D$ = −11° (*c* 0.40, MeOH); UV λ_{max} (MeOH): 202 nm (ϵ 5900); IR (film): 3374 (br), 2951 (s), 2869 (m), 1711 (s), 1454 (m), 1328 (m), 1041 (m), and 739 (m) cm^{-1}; HRFABMS: $[MNa]^+$ *m*/*z* obsd 443.2784, calcd for $C_{25}H_{40}O_5Na$ 443.2773. For ^{1}H NMR, ^{13}C NMR, HMQC, and HMBC data, see Tables 1−3.

Mangicol D (7). White amorphous solid; $[\alpha]_D$ = +76° (c 1.0, MeOH); UV λ_{max} (MeOH): 203 nm (ϵ 3000); IR (film): 3382 (br), 2940 (s), 2867 (m) cm^{-1}; HRFABMS: $[M+Na]^+$ *m*/*z* obsd 429.2987, calcd for $C_{25}H_{42}O_4Na$ 429.2981. For ^{1}H NMR, ^{13}C NMR, HMQC, and HMBC data, see Tables 1−3.

Mangicol E (8). White amorphous solid; $[\alpha]_D$ = −16° (*c* 0.42, MeOH); UV λ_{max} (MeOH): 202 nm (ϵ 5900); IR (film): 3425 (br), 2941 (s), 2867 (w), 1708 (s) cm^{-1}; HRFABMS: $[M+Na]^+$ *m*/*z* obsd 427.2829, calcd for $C_{25}H_{40}O_4Na$ 427.2824. For ^{1}H NMR, ^{13}C NMR, HMQC, and HMBC data, see Tables 1−3.

Mangicol F (9). White solid; $[\alpha]_D$ = +14° (c 0.75, MeOH); UV λ_{max} (MeOH): 202 nm (ϵ 6000); IR (film): 3430 (br), 2942 (s), 2867 (m), 1709 (s) cm^{-1}; HRFABMS: $[M+Cs]^+$ *m*/*z* obsd 521.2028, calcd for $C_{25}H_{40}O_3Na$ 521.2032. For ^{1}H NMR, ^{13}C NMR, HMQC, and HMBC data, see Tables 1−3.

Mangicol G (10). White solid; $[\alpha]_D$ = +48° (*c* 0.68, MeOH); UV λ_{max} (MeOH): 204 nm (ϵ 3200); IR (film): 3435 (br), 2938 (s), 2866 (w) cm^{-1}; HRFABMS: $[M+Cs]^+$ *m*/*z* obsd 521.2053, calcd for $C_{25}H_{40}O_3Cs$ 521.2032. For ^{1}H NMR, ^{13}C NMR, HMQC, and HMBC data, see Tables 1−3.

Diacetonide Derivative of Mangicol A (11). Mangicol A (18 mg, 0.043 mmol) was dissolved in acetone (400 μL) under argon and cooled to 0 °C. To the stirred solution was added 2,2-dimethoxypropane (DMP, 500 μL) and camphorsulfonic acid (1 mg), and the reaction mixture was stirred at 0 °C for 1 h. The reaction was quenched with 10 μL of triethylamine, concentrated under a stream of argon, dissolved in EtOAc, and passed through a small silica gel column to give a yellow oil (19 mg). Purification by HPLC (80:20 isooctane:EtOAc) afforded acetonide **11** (10.6 mg, 50%). ^{1}H NMR (600 MHz, $CDCl_3$): δ 5.48 (d, 1H, J = 1.5 Hz), 4.35 (t, 1H, J = 7.2 Hz), 4.09 (d, 1H, J = 9.0 Hz), 3.97 (d, 1H, J = 6.6 Hz), 3.72 (dd, 1H, J = 6.0, 10.8 Hz), 3.66 (d, 1H, J = 9.0 Hz), 2.42 (m, 1H), 2.25 (d, 1H, J = 14.4 Hz), 2.20 (m, 1H), 2.03 (ddd, 1H, J = 6.6, 7.8, 12.0 Hz), 2.04−1.94 (m, 2H), 1.84 (br t, 1H, J = 6.6 Hz), 1.77 (dd, 1H, J = 8.4, 15.0 Hz), 1.68 (ddd, 1H, J = 6.6, 12.0, 12.0 Hz), 1.51 (m, 1H), 1.44 (s, 3H), 1.41 (m, 1H), 1.38 (s, 3H), 1.37 (s, 3H), 1.34 (m, 1H), 1.33 (s, 3H), 1.32 (s, 3H), 1.18 (q, 1H, J = 11.4 Hz), 1.13 (s, 3H), 1.10 (d, 3H, J = 7.2 Hz), 0.92 (s, 3H), and 0.89 (d, 3H, J = 7.2 Hz); ^{13}C NMR (100 MHz, $CDCl_3$): δ 141.2, 133.0, 109.8, 107.1, 83.1, 81.7, 81.0, 75.5, 74.7, 58.3, 57.2, 46.4, 43.8, 42.7, 39.6 (2), 37.7, 34.2, 34.0, 33.2, 33.0, 30.3, 27.4, 27.1, 26.9, 24.8, 23.6, 21.5, 21.3, and 21.0.

Preparation of Mosher Ester 12. Diacetonide **11** (7.8 mg, 0.016 mmol) was dissolved in CH_2Cl_2 (200 μL) under argon. Added to the stirred solution were DMAP (1 mg), pyridine (10 μL), and (*R*)-MTPA-Cl (12 μL, 0.064 mmol). The reaction mixture was stirred at room temperature for 72 h, concentrated under argon, and quenched with 1 M NH_4Cl (500 μL)

for 25 min. The mixture was extracted with CH_2Cl_2 (3 × 3 mL), dried over $MgSO_4$, and concentrated to give a yellow oil (17.7 mg). Purification by silica gel HPLC (80:20 isooctane:EtOAc) afforded ester **12** (6.1 mg). ^{1}H NMR (500 MHz, $CDCl_3$): δ 7.56−7.54 (m, 2H), 7.43−7.39 (m, 3H), 5.54 (d, 1H, J = 2.0 Hz), 4.82 (dd, 1H, J = 6.5, 11.0 Hz), 4.32 (ddd, 1H, J = 1.0, 6.5, 6.5 Hz), 4.10 (d, 1H, J = 9.0 Hz), 3.96 (d, 1H, J = 6.5 Hz), 3.65 (d, 1H, J = 8.0 Hz), 3.62 (s, 3H), 2.53 (m, 1H), 2.38 (ddd, 1H, J = 6.5, 8.0, 12.0 Hz), 2.20 (dd, 1H, J = 1.0, 15.5 Hz), 2.16 (m, 1H), 1.70 (dd, 1H, J = 8.5, 15.0 Hz), 1.62−1.54 (m, 3H), 1.52−1.38 (m, 2H), 1.45 (s, 3H), 1.38 (s, 3H), 1.36 (s, 3H), 1.33 (s, 3H), 1.32 (s, 3H), 1.32−1.16 (m, 2H), 1.14 (d, 3H, J = 7.5 Hz), 1.10 (s, 3H), 0.87 (s, 3H), 0.83 (d, 3H, J = 7.0 Hz).

Preparation of Mosher Ester 13. Diacetonide **11** (8.5 mg, 0.017 mmol) was dissolved in CH_2Cl_2 (200 μL) under argon. Added to the stirred solution were DMAP (1 mg), pyridine (10 μL), and (*S*)-MTPA-Cl (15 μL, 0.080 mmol). The reaction mixture was stirred at room temperature for 72 h. TLC analysis at this time showed little reaction had occurred. An additional 20 μL of MTPA-Cl was added, and the reaction mixture was stirred for 24 h at room temperature, followed by 72 h at 60 °C. The mixture was concentrated under argon and quenched with 1 M NH_4Cl (500 μL) for 25 min. The mixture was extracted with CH_2Cl_2 (3 × 5 mL), dried over $MgSO_4$, and concentrated to give a yellow oil (40 mg). Purification by silica gel HPLC (80:20 isooctane:EtOAc) afforded ester **12** (3.3 mg). ^{1}H NMR (500 MHz, $CDCl_3$): δ 7.53−7.50 (m, 2H), 7.44−7.41 (m, 3H), 5.54 (d, 1H, J = 2.0 Hz), 4.80 (dd, 1H, J = 6.0, 11.5 Hz), 4.33 (ddd, 1H, J = 1.0, 6.5, 6.5 Hz), 4.10 (d, 1H, J = 9.0 Hz), 3.97 (d, 1H, J = 6.5 Hz), 3.65 (d, 1H, J = 8.0 Hz), 3.49 (s, 3H), 2.52 (m, 1H), 2.38 (ddd, 1H, J = 6.0, 8.0, 12.0 Hz), 2.23 (dd, 1H, J = 1.0, 15.0 Hz), 2.12 (m, 1H), 1.74 (dd, 1H, J = 8.5, 15.0 Hz), 1.80−1.66 (m, 3H), 1.54−1.35 (m, 2H), 1.44 (s, 3H), 1.38 (s, 3H), 1.36 (s, 3H), 1.33 (s, 6H), 1.32−1.16 (m, 2H), 1.12 (d, 3H, J = 7.5 Hz), 1.11 (s, 3H), 0.91 (s, 3H), 0.83 (d, 3H, J = 7.0 Hz).

Acknowledgment. This work was supported by the National Institutes of Health, National Cancer Institute, through Grants CA44848 and CA50560. We greatly appreciate technical assistance from Mr. Chris Kauffman and Dr. Alan Deese. Mass spectral analyses were performed at The Scripps Research Institute Mass Spectrometry Facility. We thank Professor David Porter, University of Georgia, for tentative identification of this fungal strain and Professor Robert Jacobs for providing antiinflammatory testing.

Supporting Information Available: Figures showing spectral data for mangicols A−G (S1−S56). This material is available free of charge via the Internet at http://pubs.acs.org.

JO000081H